



Superconducting Qubits

Lecture 4

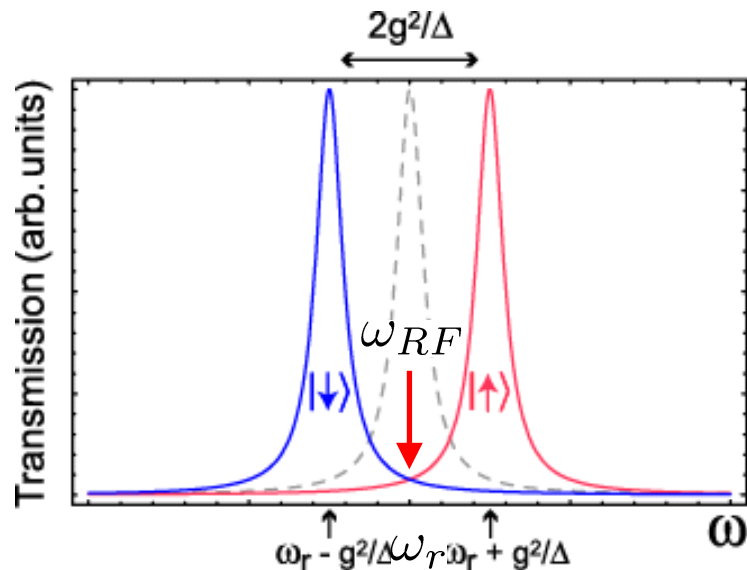
Non-Resonant Coupling for Qubit Readout

approximate diagonalization for $|\Delta| = |\omega_a - \omega_r| \gg g$

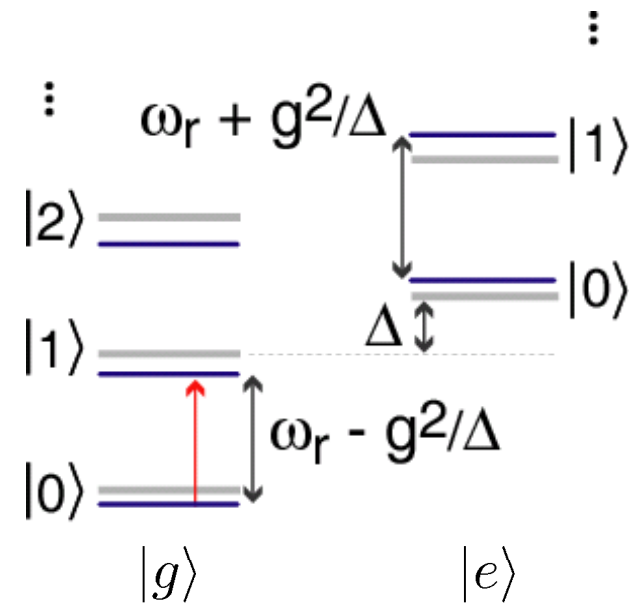
$$H \approx \hbar \left(\omega_r + \frac{g^2}{\Delta} \sigma_z \right) a^\dagger a + \frac{1}{2} \hbar \left(\omega_a + \frac{g^2}{\Delta} \right) \sigma_z$$

//

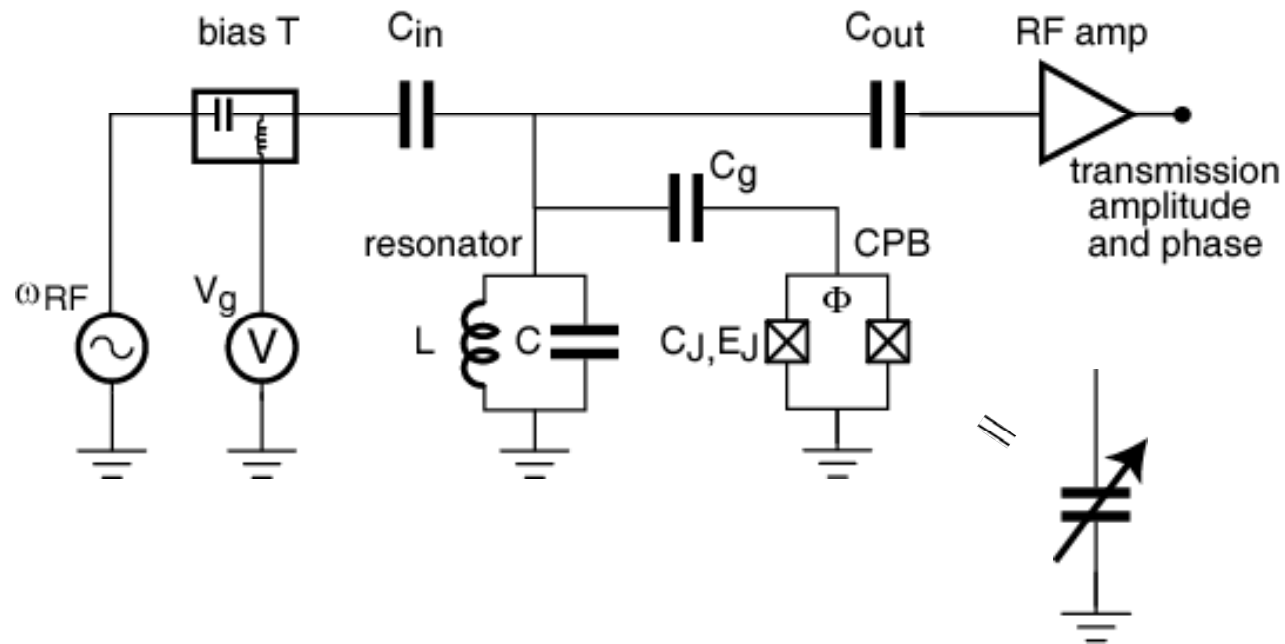
cavity frequency shift
and qubit ac-Stark shift



dispersive level diagram:



Measurement Technique

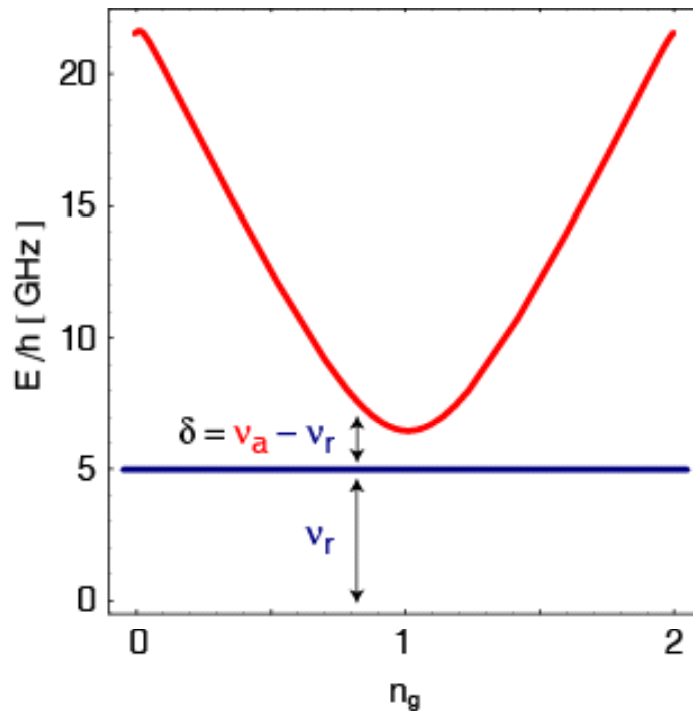


- measurement of microwave transmission amplitude T and phase ϕ
- intra-cavity photon number controllable from $n \sim 10^3$ to $n \ll 1$

Dispersive Shift of Resonance Frequency

sketch of qubit level separation:

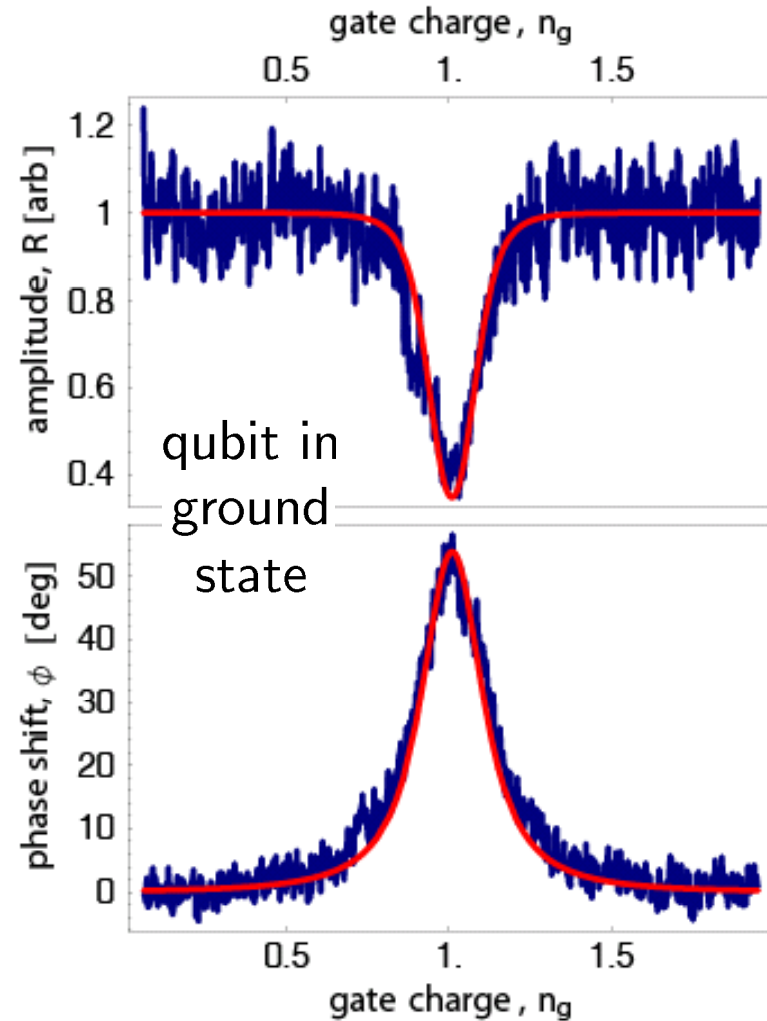
$$\Delta = 2\pi\delta > g$$



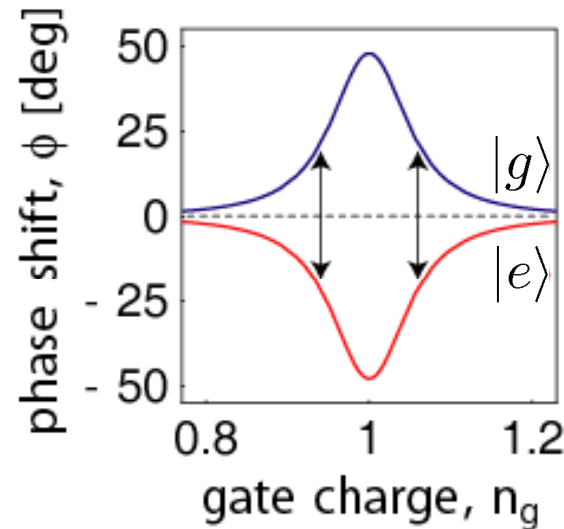
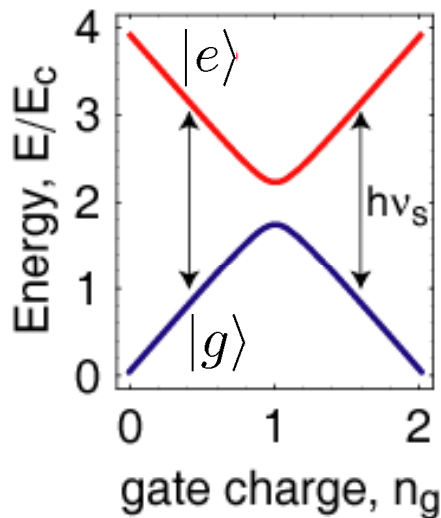
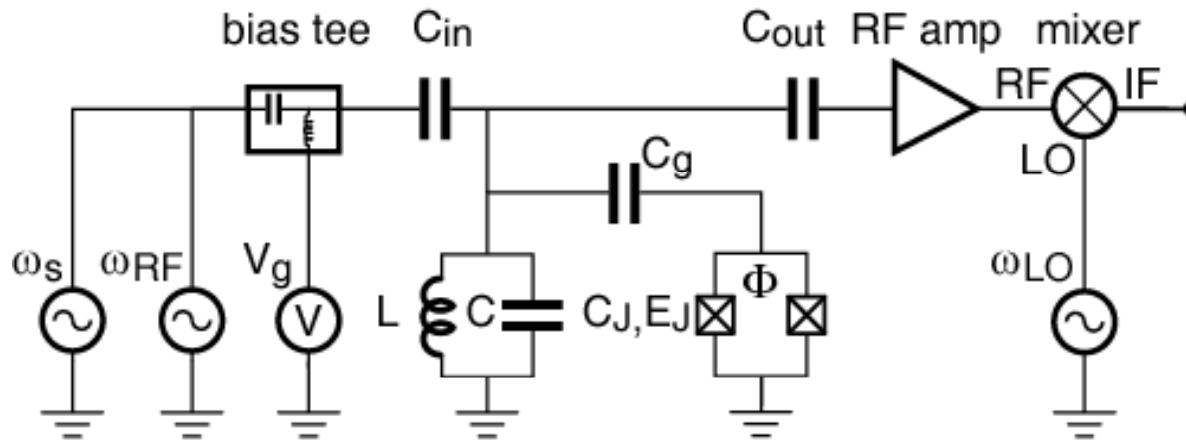
$$g/\pi = \nu_{\text{vac}} = 11 \text{ MHz}$$
$$\Delta(n_g = 1)/2\pi = 66 \text{ MHz}$$

$$n = 10$$

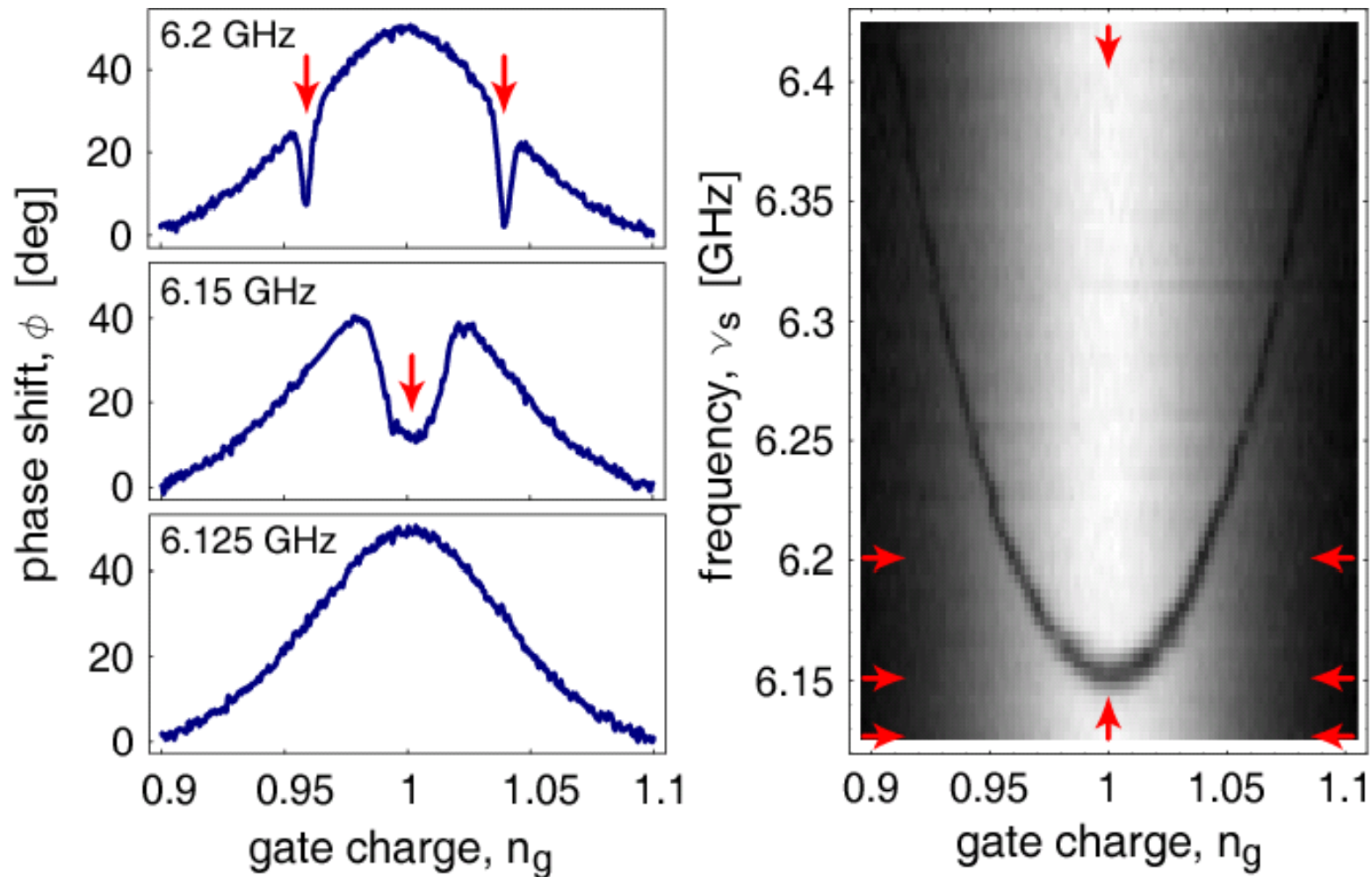
measured resonator transmission amplitude and phase:



Qubit Spectroscopy with Dispersive Read-Out



CW Spectroscopy of Cooper Pair Box



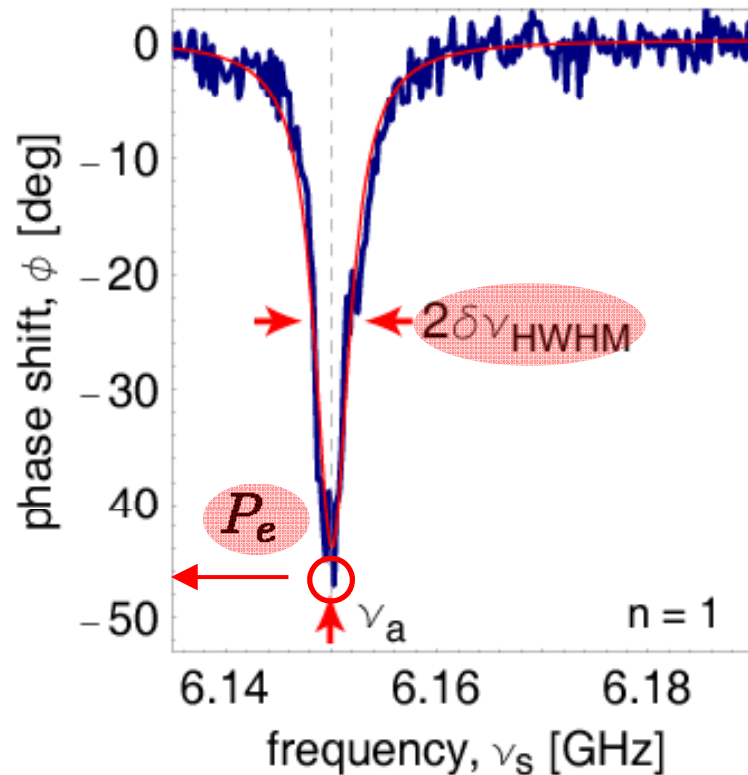
detuning $\Delta_{r,a}/2\pi \sim 100$ MHz

extracted: $E_J = 6.2$ GHz, $E_C = 4.8$ GHz

Line Shape

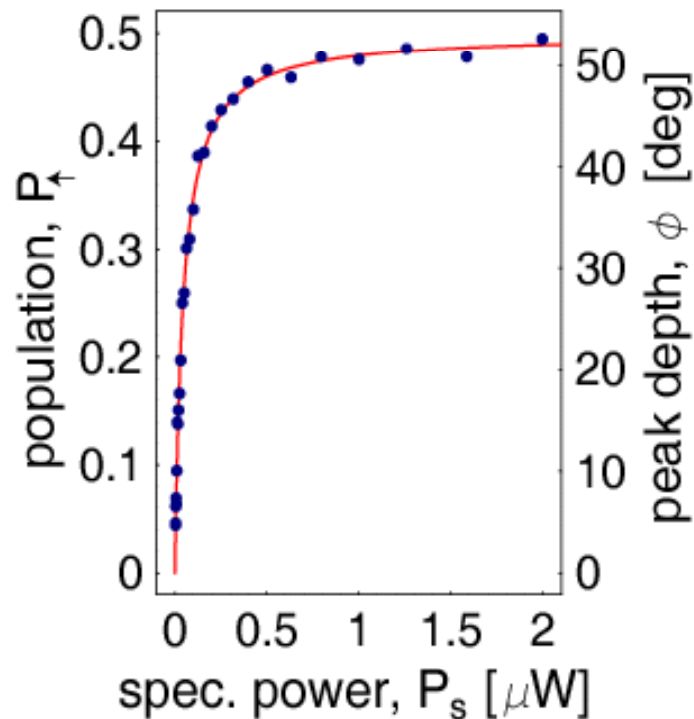
excited state population (steady-state Bloch equations):

$$P_e = 1 - P_g = \frac{1}{2} \frac{\Omega_R^2 T_1 T_2}{1 + (T_2 \Delta_{s,a})^2 + \Omega_R^2 T_1 T_2}$$



- fixed drive $P_s \propto \Omega_R^2 = n_s \omega_{\text{vac}}^2$
- varying $\Delta_{s,a} = \omega_s - \tilde{\omega}_a$
- weak continuous measurement ($n \sim 1$)
- at charge degeneracy ($n_g = 1$)

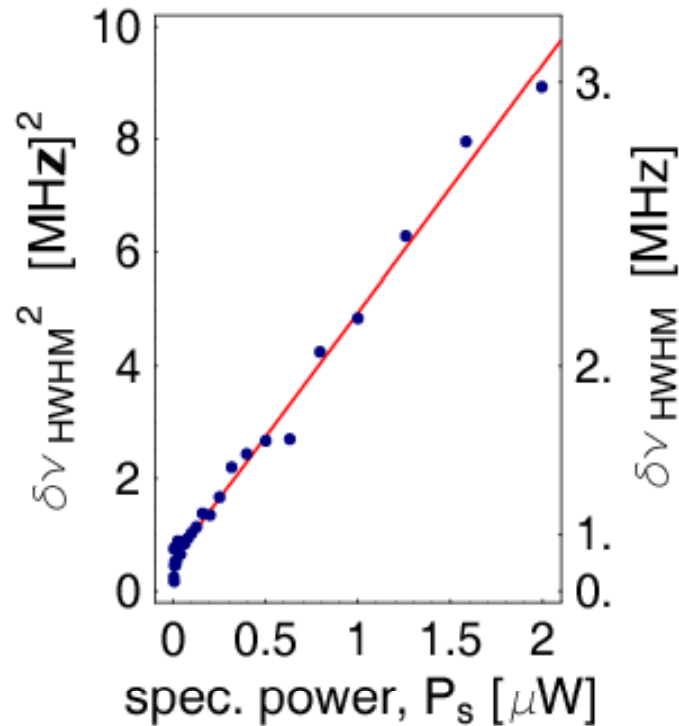
Excited State Population



peak depth \rightarrow population (saturation):

$$P_e = 1 - P_g = \frac{1}{2} \frac{\Omega_R^2 T_1 T_2}{1 + \Omega_R^2 T_1 T_2}$$

Line Width

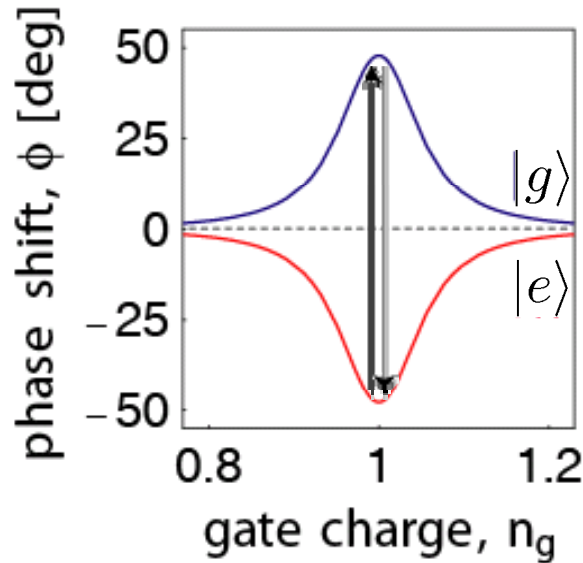
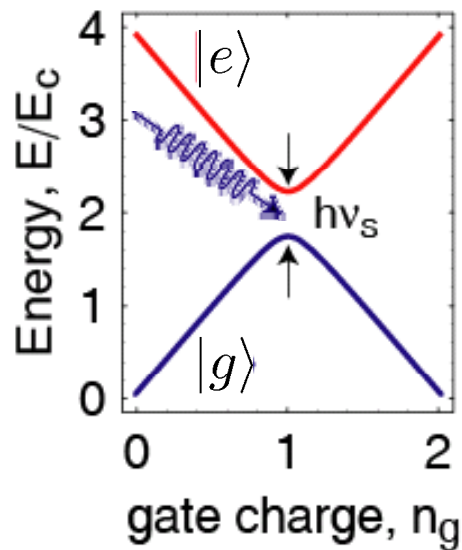


line width \rightarrow coherence time:

$$2\pi\delta\nu_{\text{HWHM}} = \frac{1}{T_2'} = \sqrt{\frac{1}{T_2^2} + \Omega_R^2 \frac{T_1}{T_2}}$$

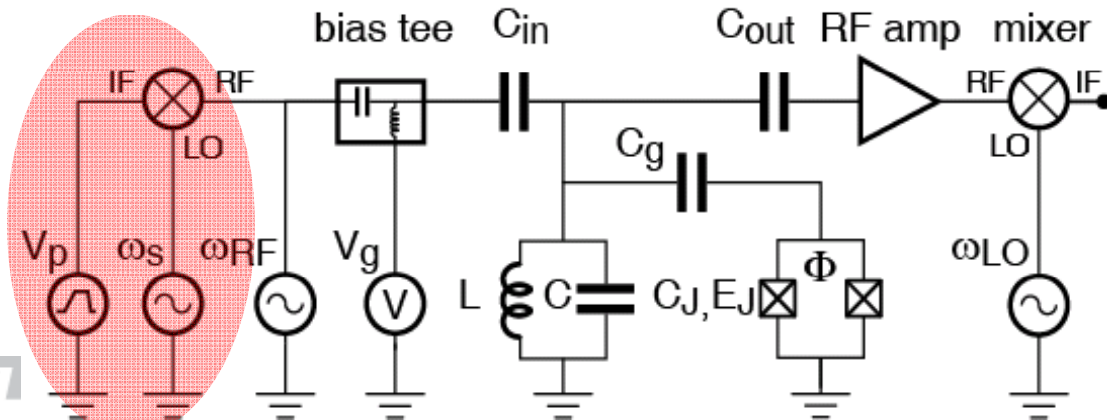
$\text{Min}(\delta\nu_{\text{HWHM}}) \sim 750 \text{ kHz} \rightarrow T_2 > 200 \text{ ns}$

Coherent Control and Readout in a Cavity



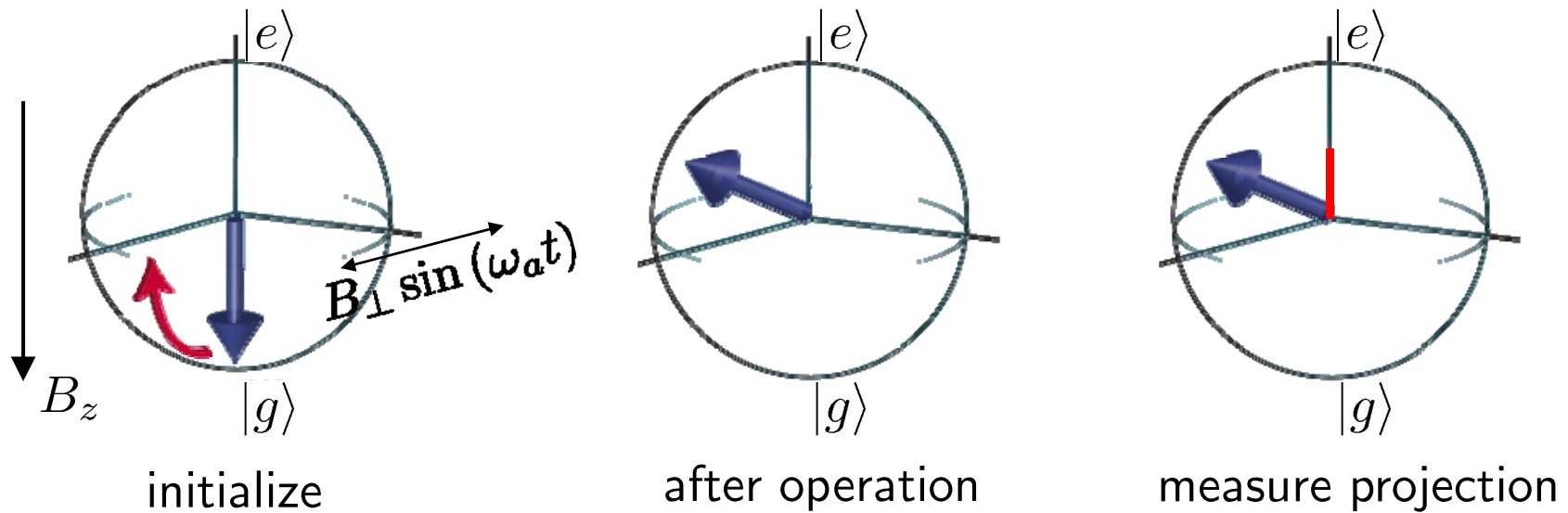
- apply resonant microwave pulse to qubit
- detect change of phase

realization:



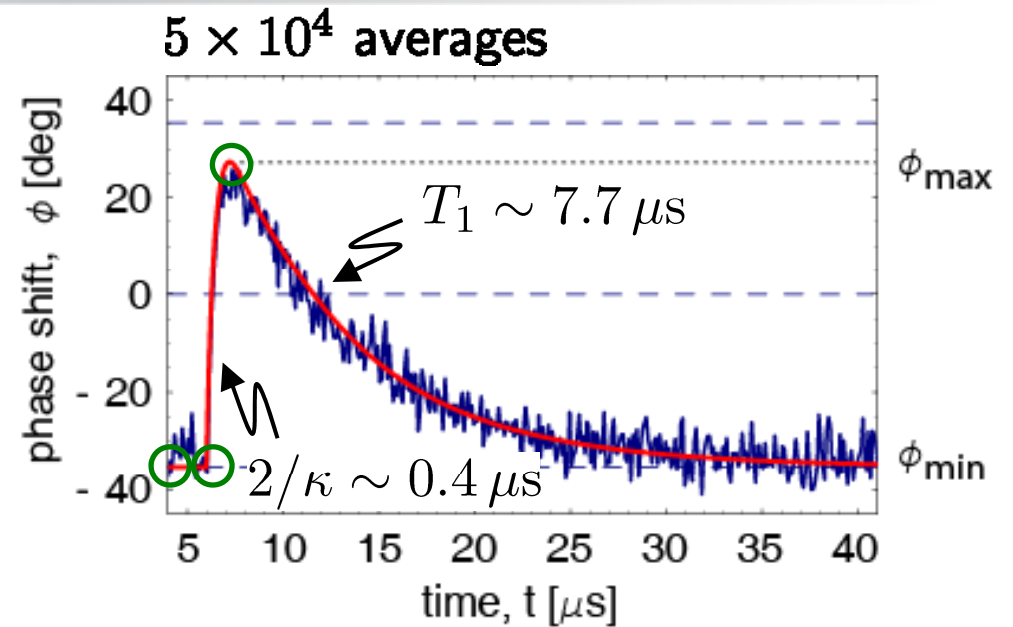
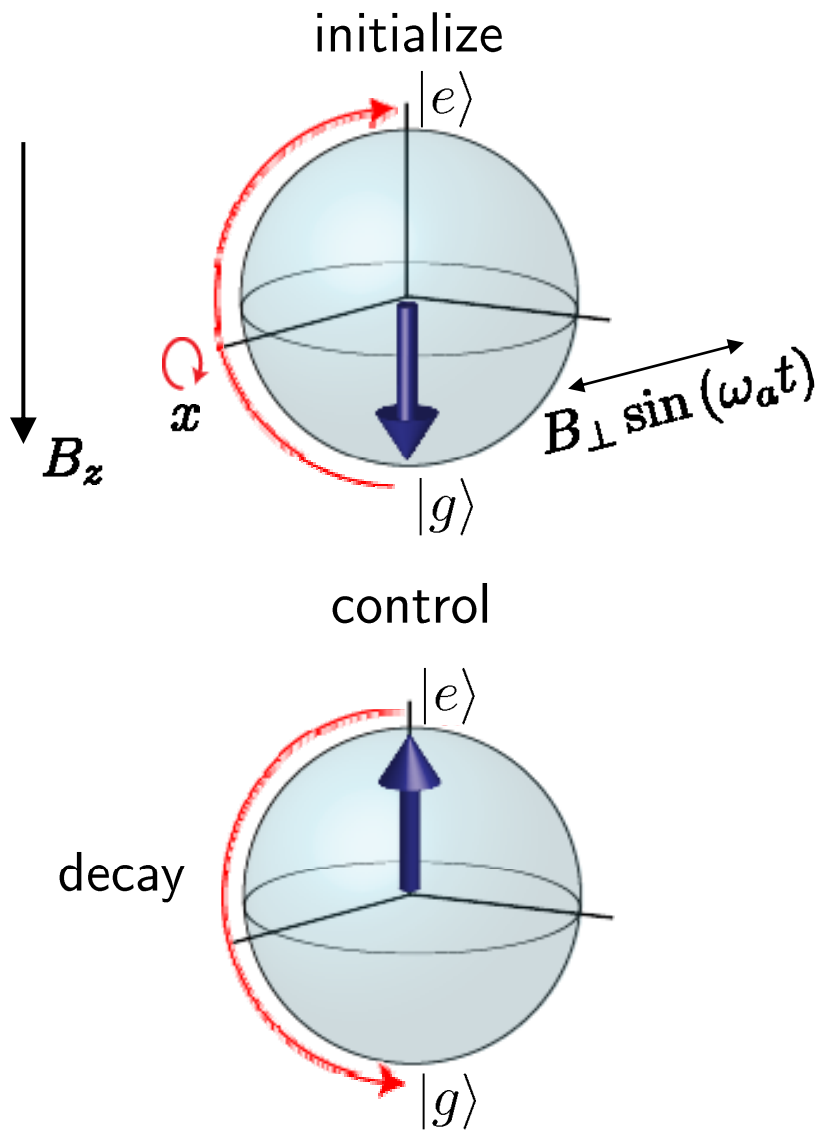
- simultaneous control and measurement

Coherent Control of a Qubit in a Cavity



- qubit state represented on a Bloch sphere
- vary length, amplitude and phase of microwave pulse to control qubit state

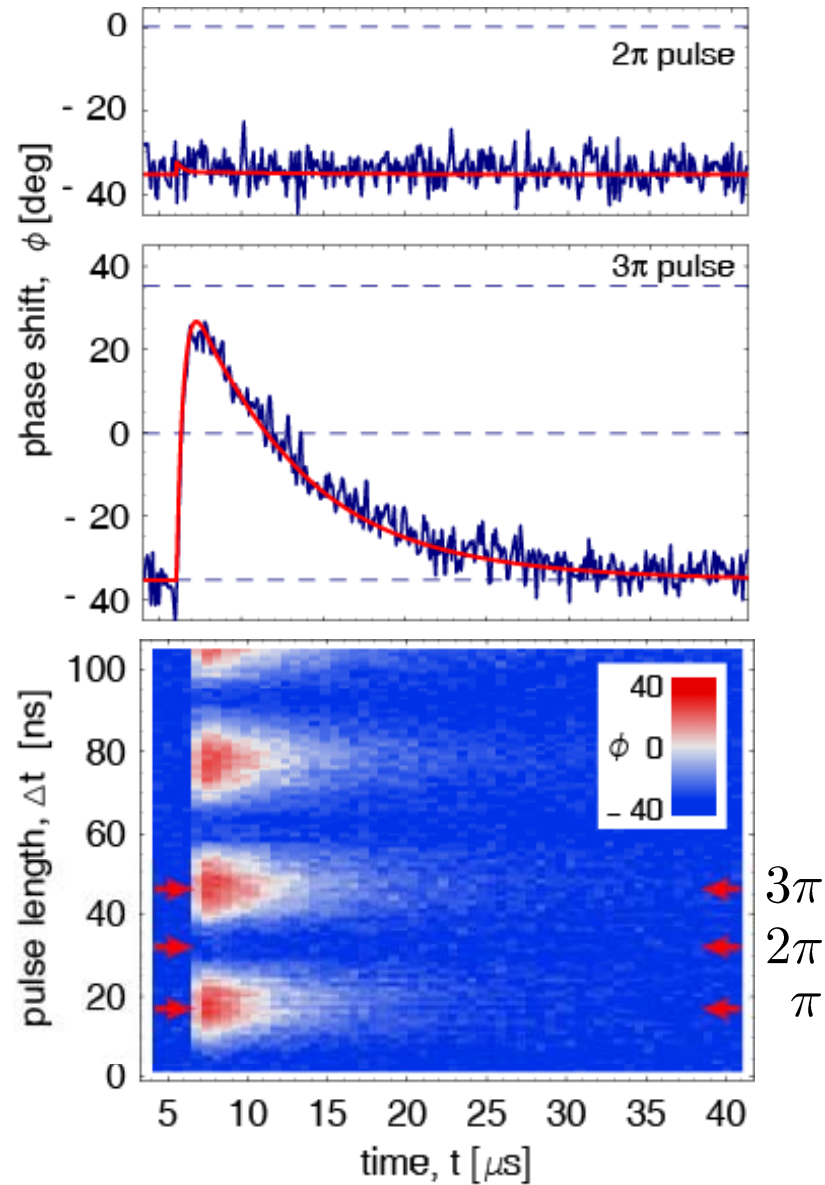
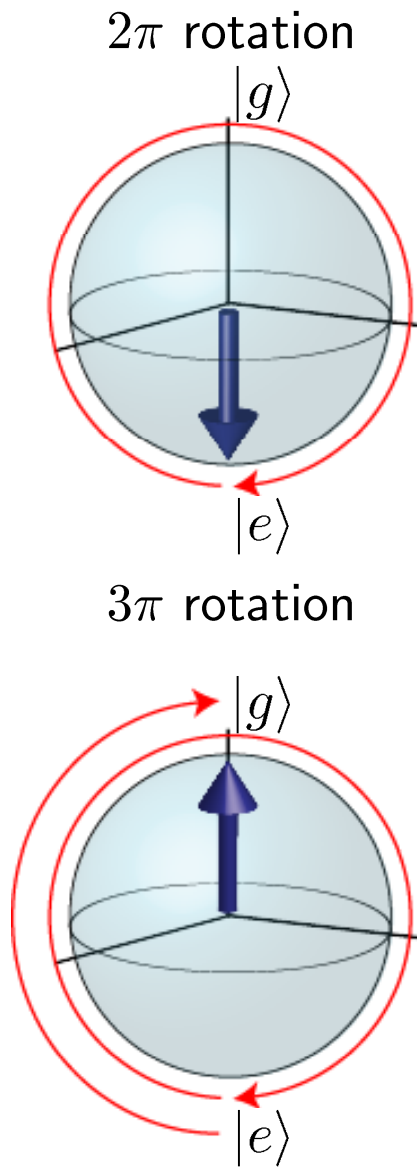
Qubit Control and Readout



measurement properties:

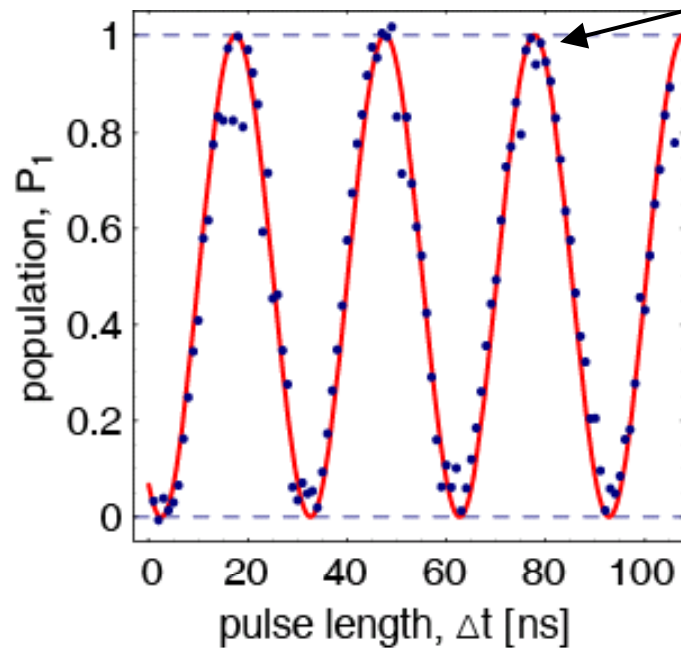
- continuous
- dispersive
- quantum non-demolition
- in good agreement with predictions

Varying the Control Pulse Length



High Visibility Rabi Oscillations

Rabi oscillations:



visibility $95 \pm 5\%$

for superconducting qubits:

- high visibility
- well characterized and understood measurement
- good control accuracy

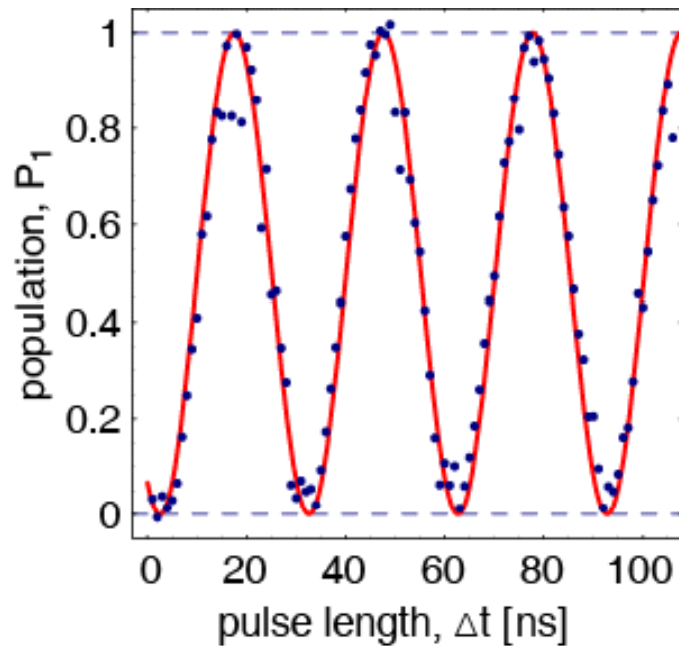
A. Wallraff, D. I. Schuster, A. Blais, L. Frunzio,
J. Majer, S. M. Girvin, and R. J. Schoelkopf,
Phys. Rev. Lett. **95**, 060501 (2005)

Rabi Frequency

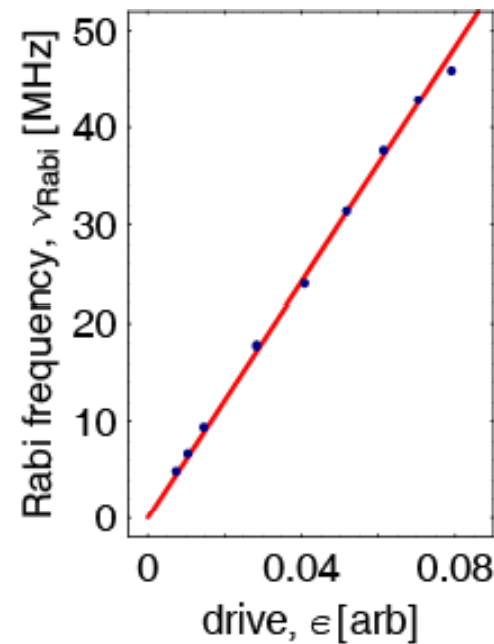
pulse scheme:



Rabi oscillations:

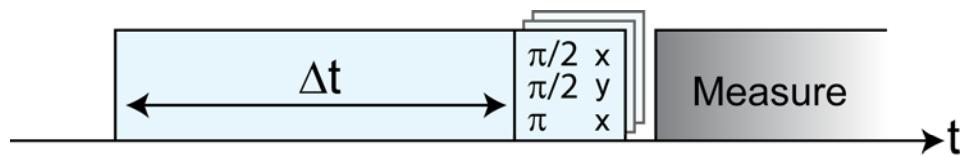


Rabi frequency:

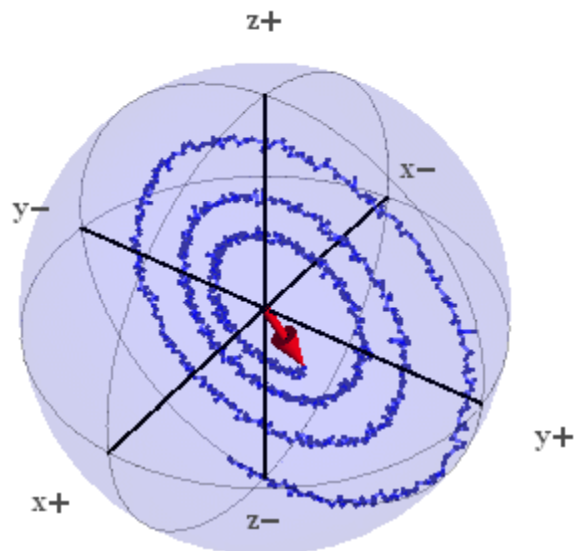


- linear dependence of Rabi frequency on microwave amplitude

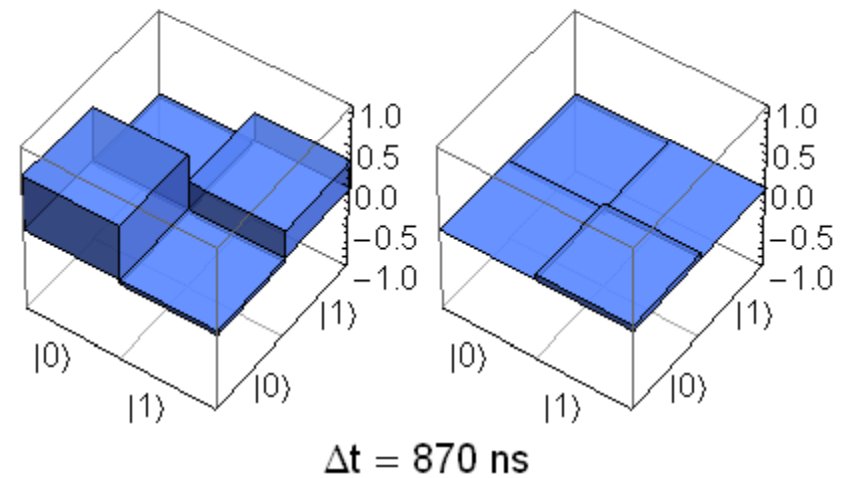
Rabi rotation pulse sequence:



experimental Bloch vector:



experimental density matrix:



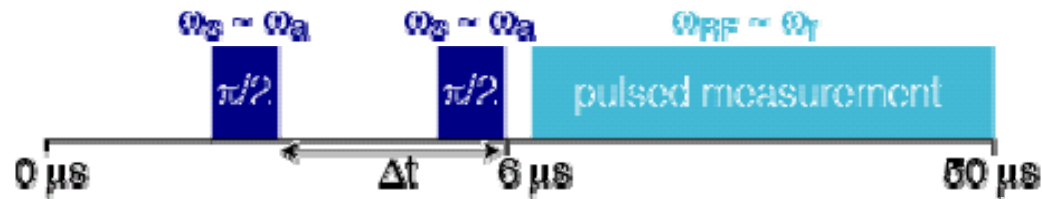
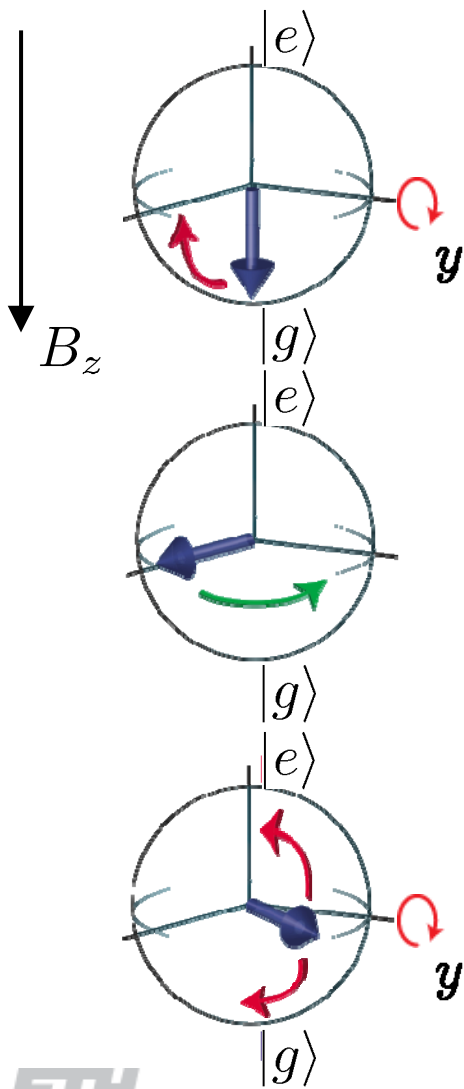


Measurements of Coherence Time

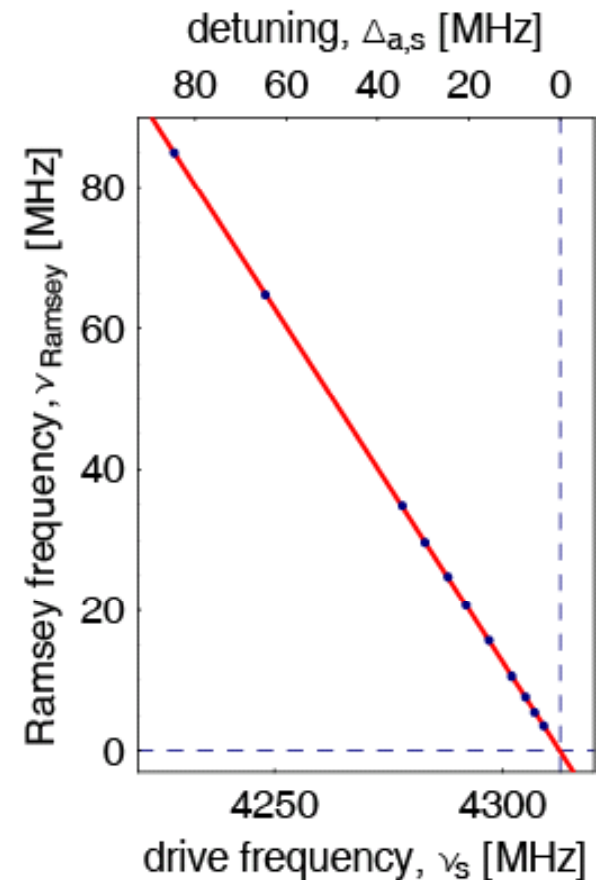
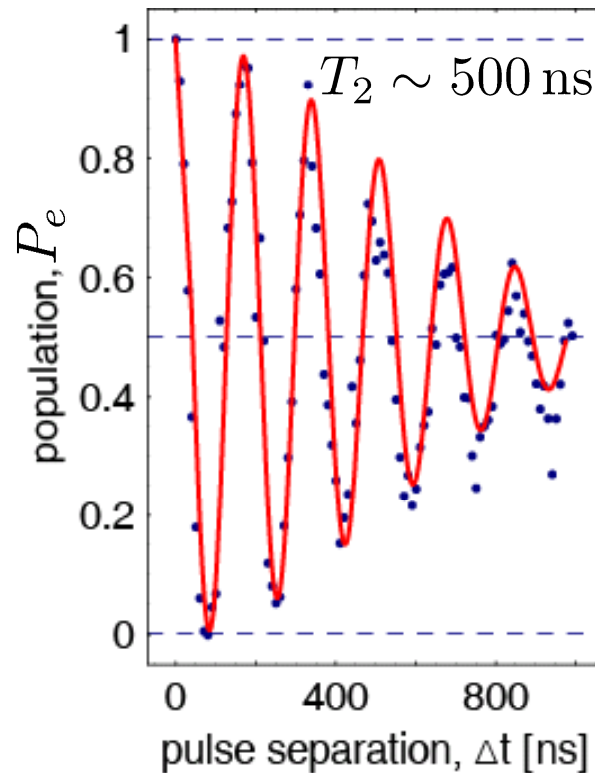


Coherence Time Measurement: Ramsey Fringes

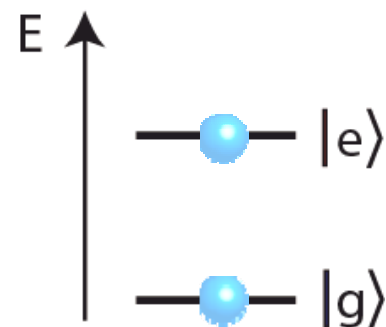
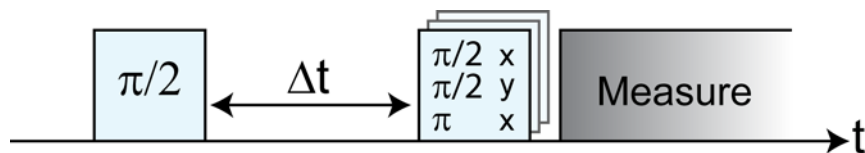
pulse scheme:



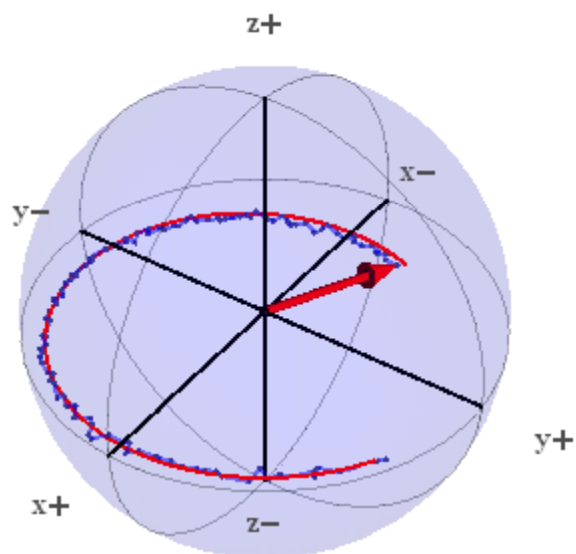
Ramsey fringes:



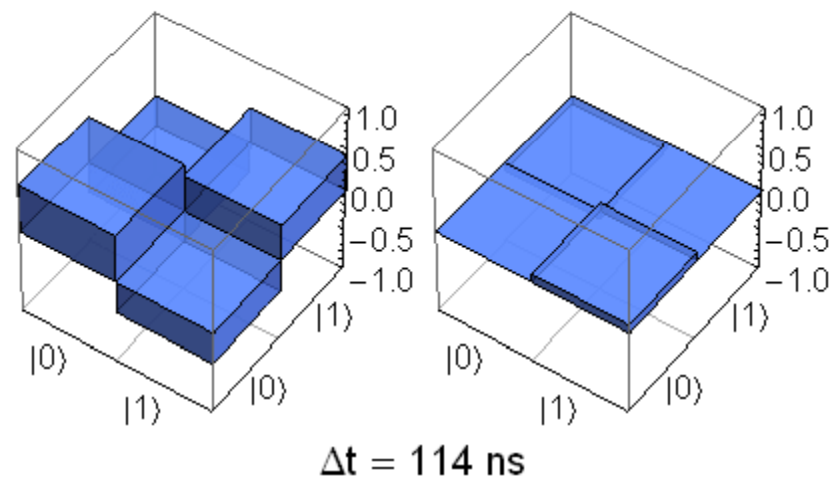
pulse sequence:



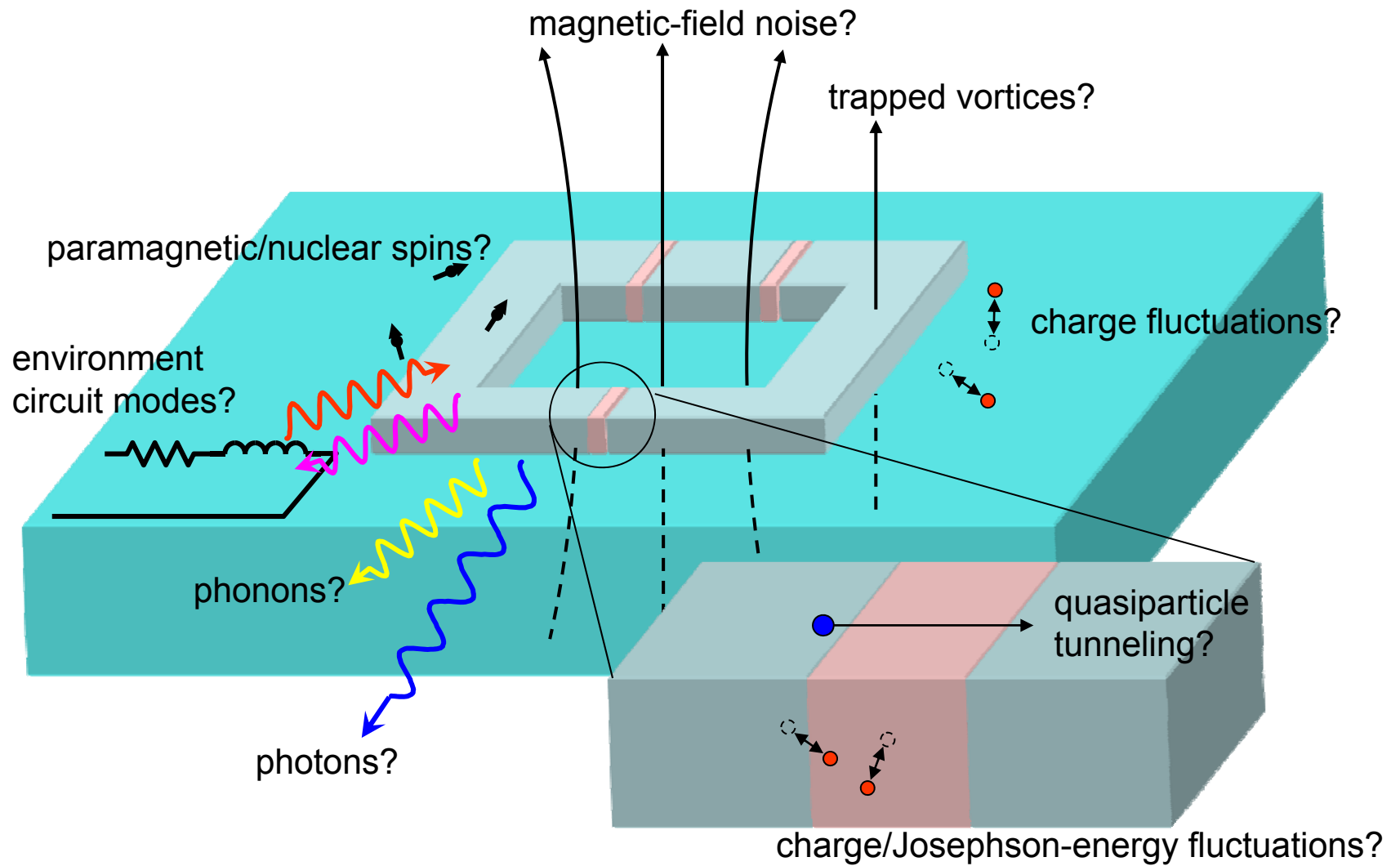
experimental Bloch vector:



experimental density matrix:

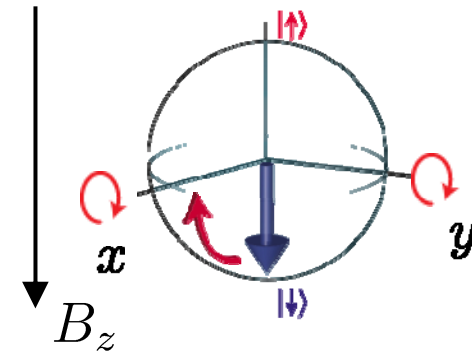
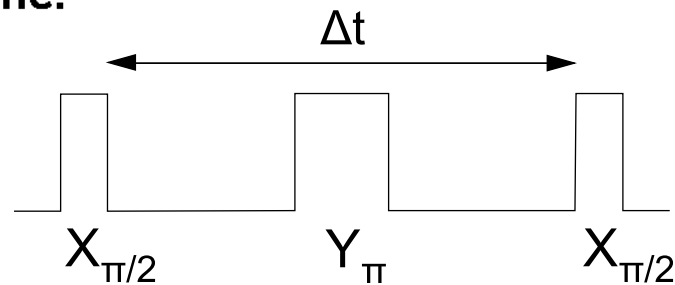


Sources of Decoherence

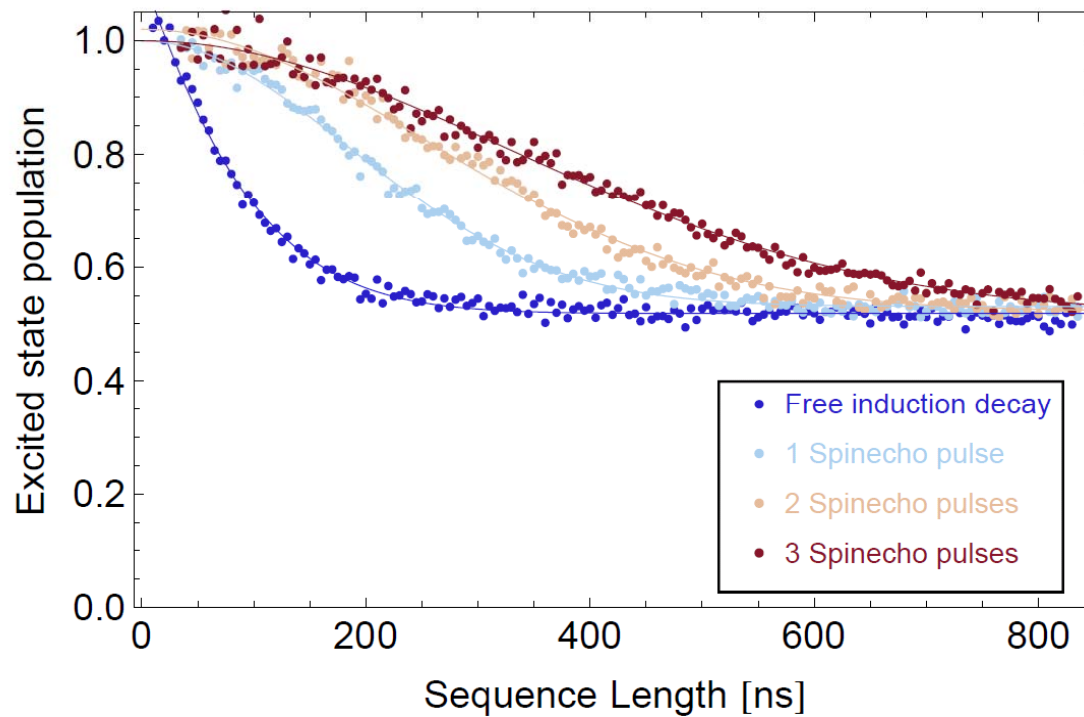


-
- remove sources of decoherence
 - improve materials
 - use dynamic methods to counteract specific sources of decoherence
 - spin echo
 - geometric manipulations
 - reduce sensitivity of quantum systems to specific sources of decoherence
 - make use of symmetries in design and operation

pulse scheme:



result:

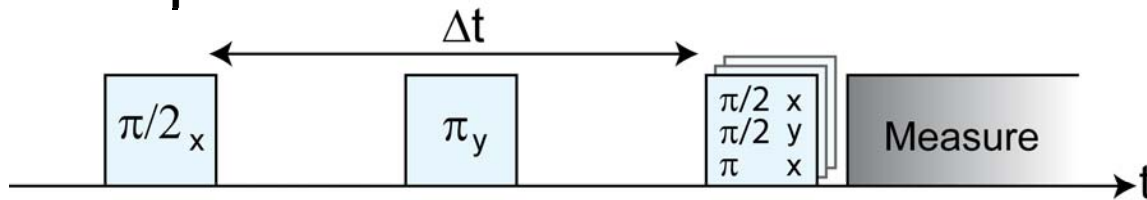


- refocusing
- elimination of low frequency fluctuations
- increased effective coherence time

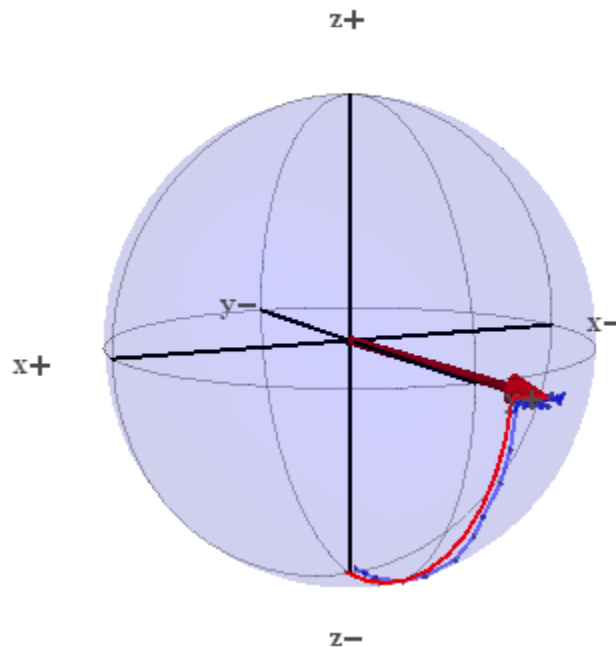


Tomography of a Spin Echo

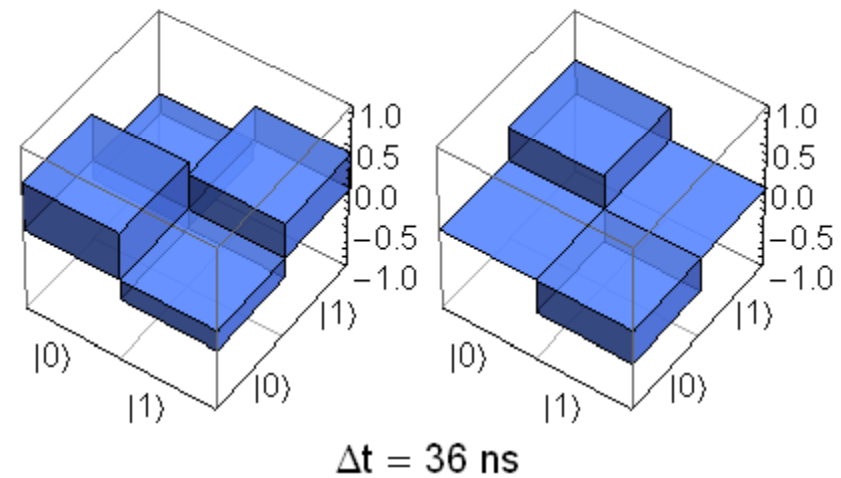
pulse sequence:




experimental Bloch vector:



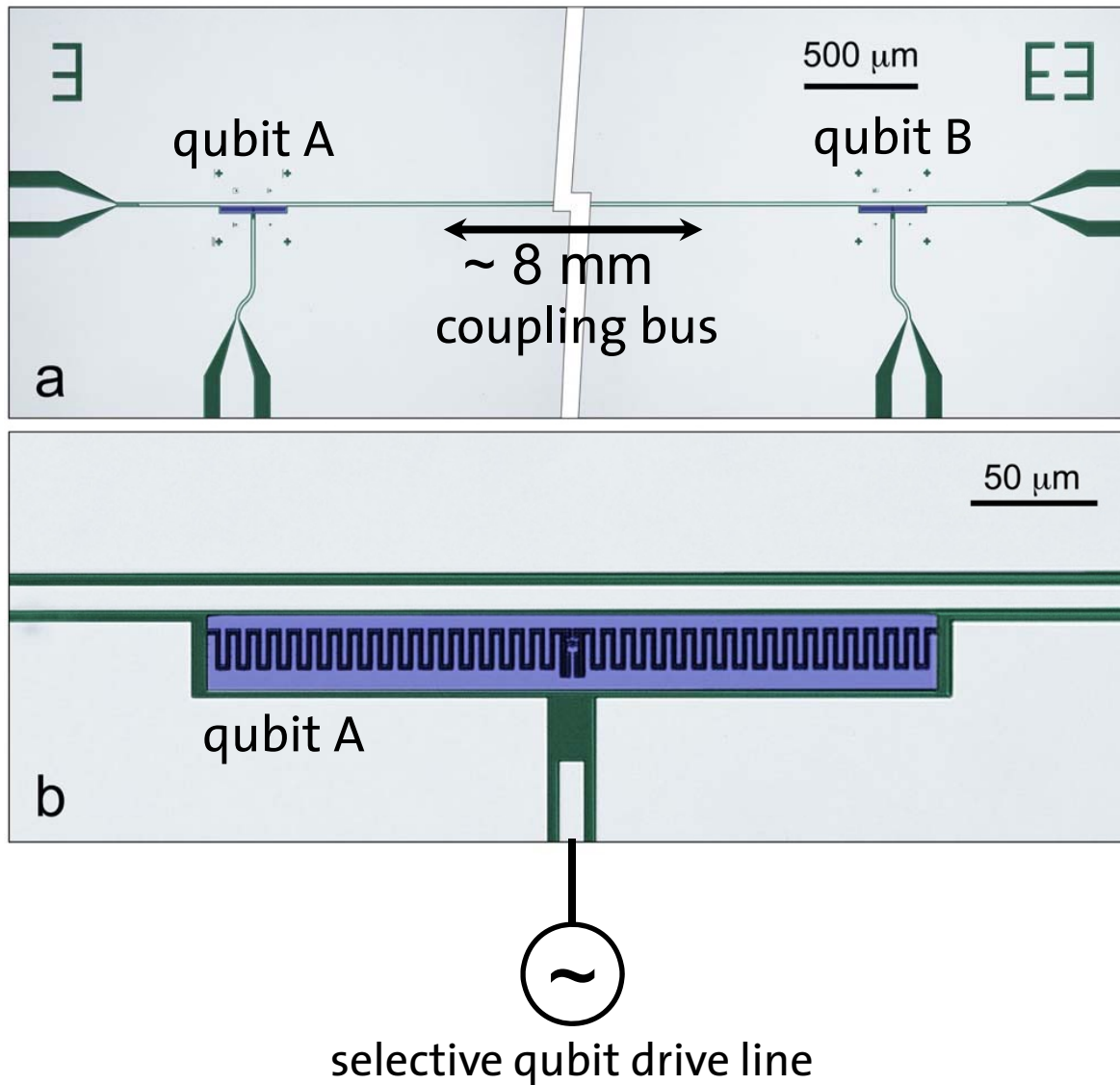
experimental density matrix:





Coupling Superconducting Qubits and Generating Entanglement using Sideband Transitions

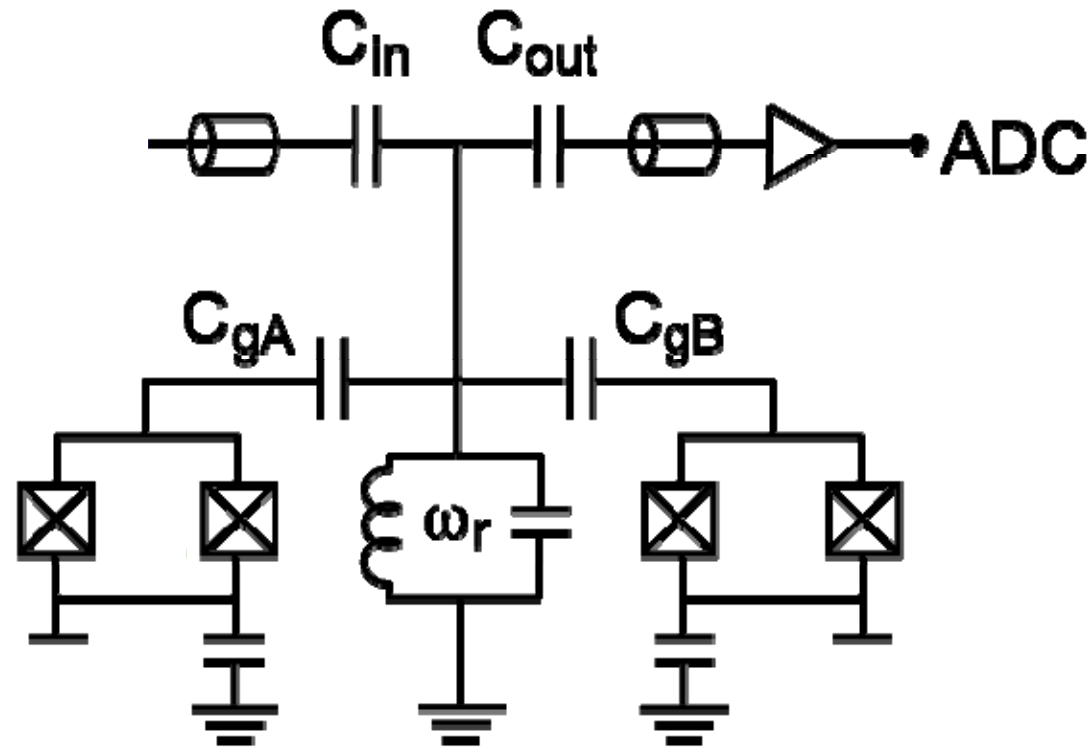
2-Qubit Chip



- Two near identical superconducting qubits
- Local control of magnetic flux allows independent selection of qubit transition frequencies
- Local drive lines allow selective excitation of individual qubits

2-Qubit Circuit with Selective Control

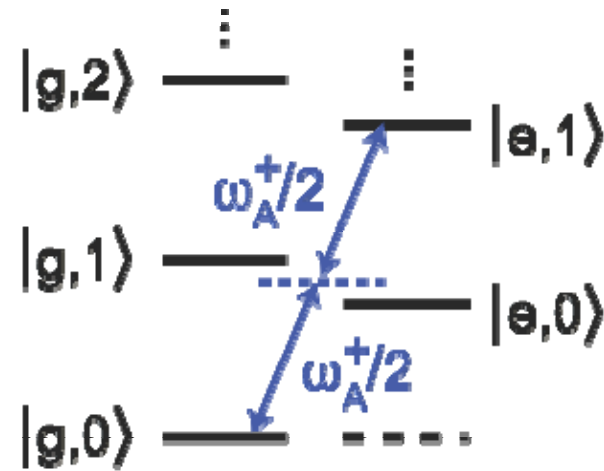
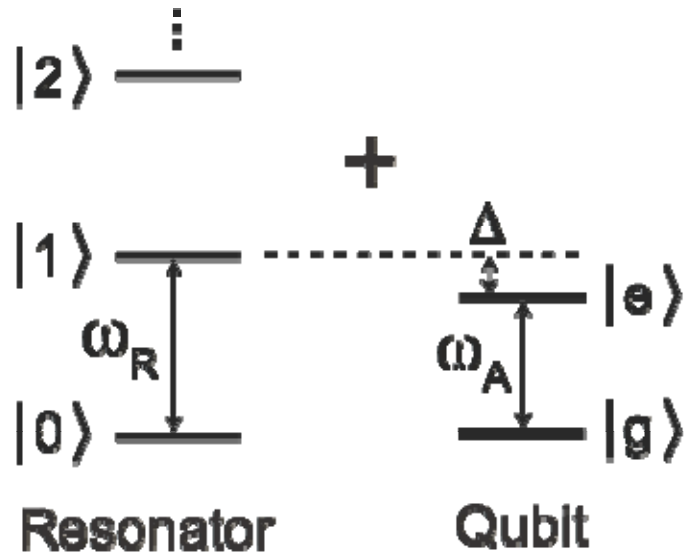
joint dispersive
read-out



Local magnetic
fields created
using small
inductively
coupled coils

Selective qubit excitation
using locally capacitively
coupled drive lines

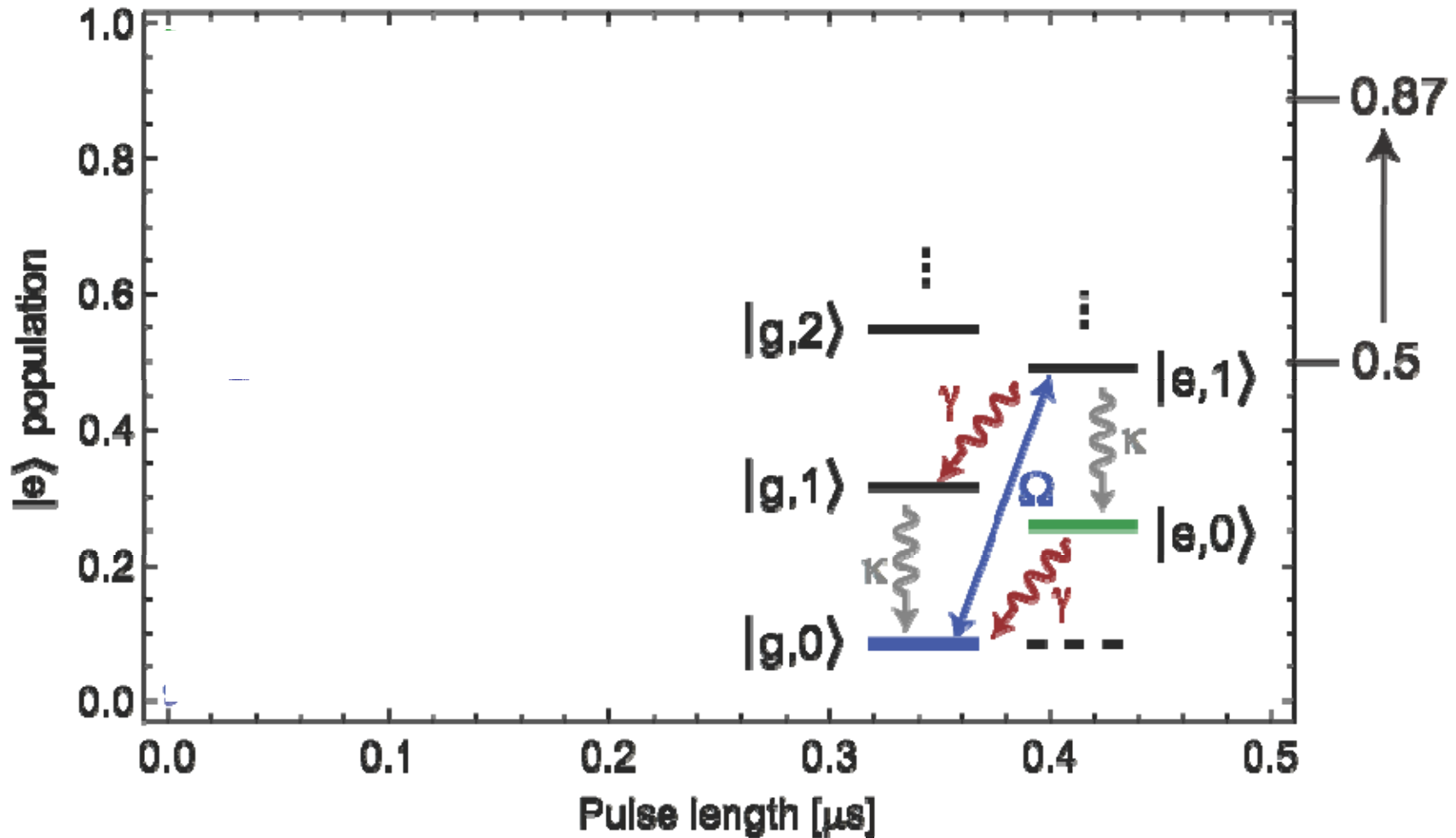
Sideband Transitions in Circuit QED



$$\omega_A^+/2 = (\omega_R + \omega_A)/2$$

- ▶ dispersive coupling allows joint excitations to be driven
- ▶ sideband transitions forbidden to first order: use two photon transition

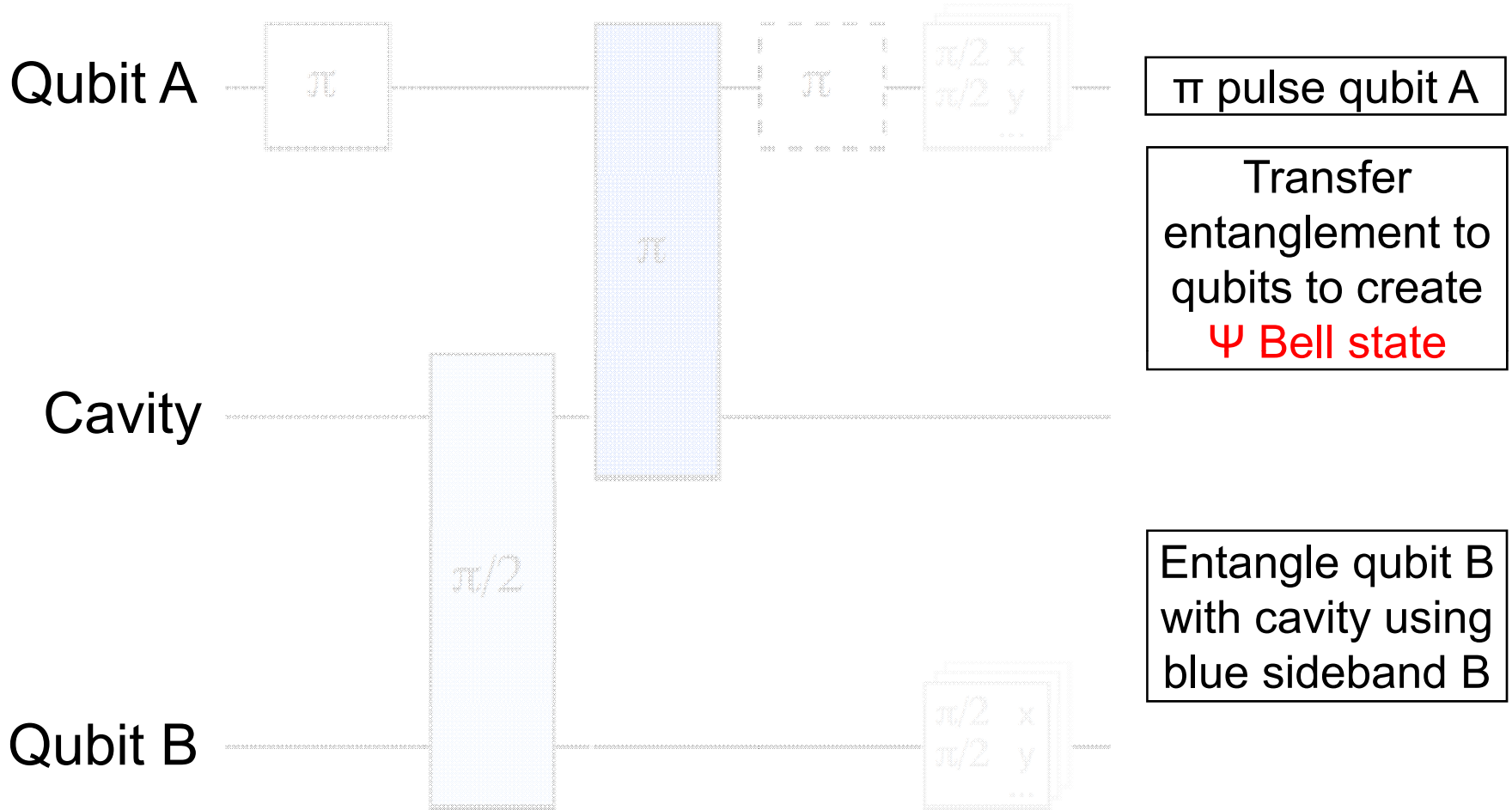
/Resonator Sideband Transitions



simultaneous excitation of qubit and resonator: $|g,0\rangle \rightarrow |e,1\rangle$

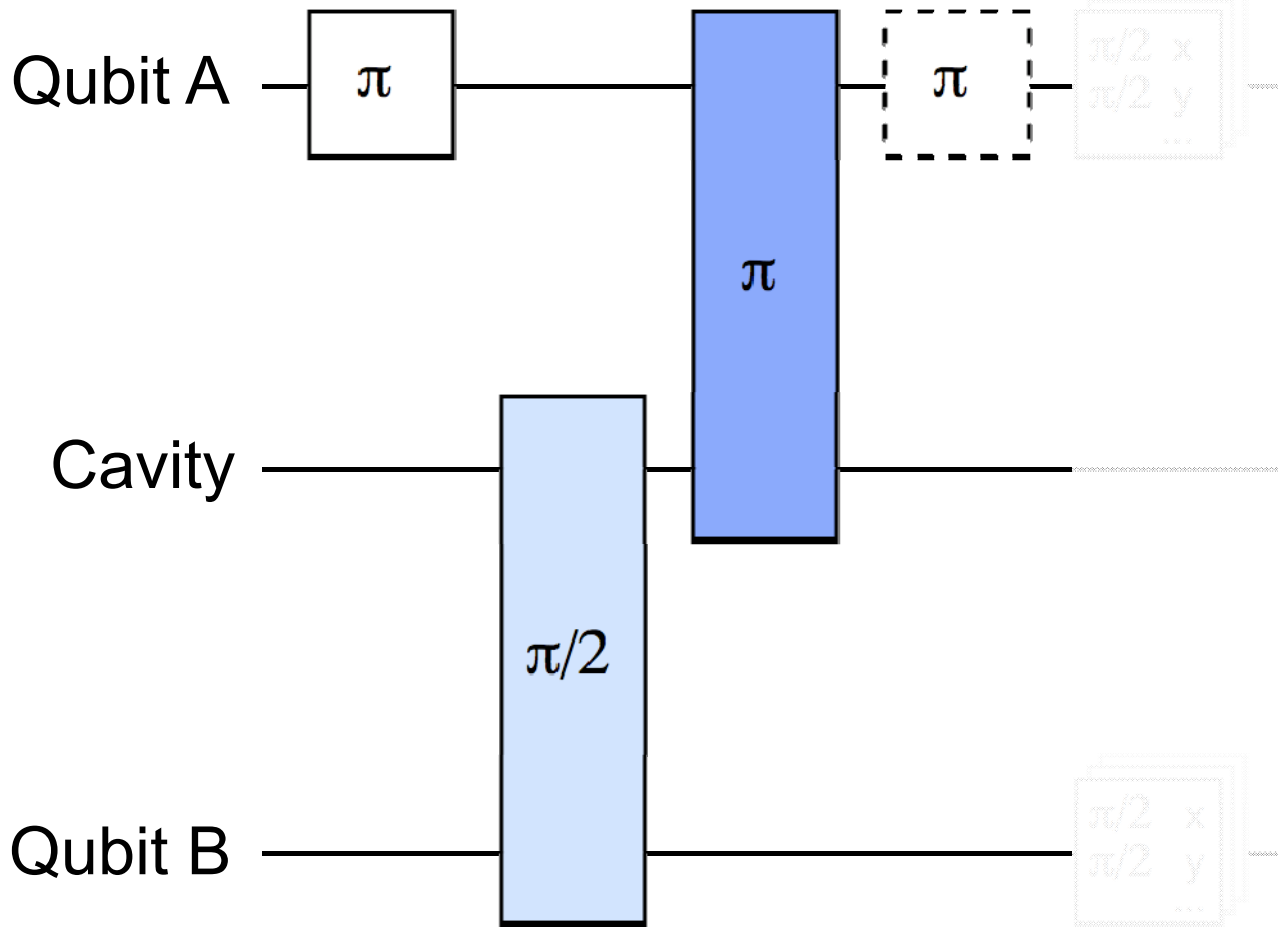
entangle a qubit with a photon on the bus: $|g,0\rangle \rightarrow |g,0\rangle + |e,1\rangle$

Bell State Preparation



$$|gg0\rangle \longrightarrow |eg0\rangle \longrightarrow \frac{1}{\sqrt{2}}(|eg0\rangle + |ee1\rangle) \longrightarrow \frac{1}{\sqrt{2}}(|eg\rangle + |ge\rangle) \otimes |0\rangle$$

Bell State Preparation



π pulse qubit A to convert to Φ Bell state

π pulse qubit A

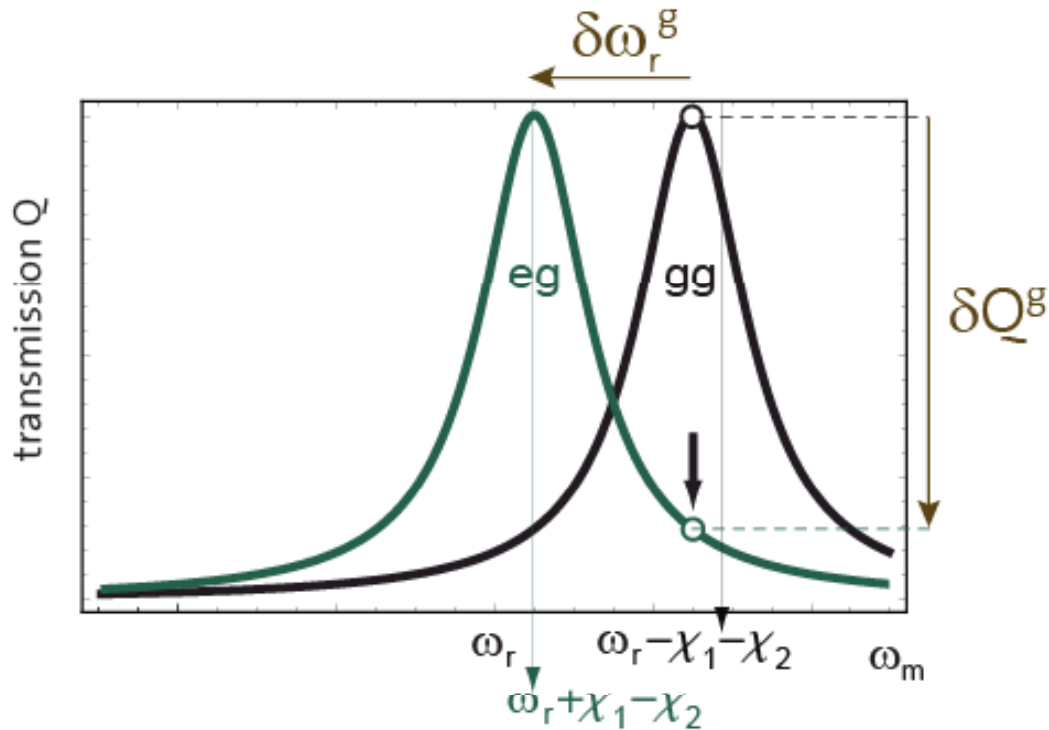
Transfer entanglement to qubit A to create Ψ Bell state

Characterise the entanglement of qubit B with cavity state to the graph with joint msrmt

$$\dots \rightarrow \frac{1}{\sqrt{2}}(|eg\rangle + |ge\rangle) \otimes |0\rangle \rightarrow \frac{1}{\sqrt{2}}(|gg\rangle + |ee\rangle) \otimes |0\rangle$$

Joint Two Qubit Readout

Amplitude difference (δQ) depends on state of both qubits:



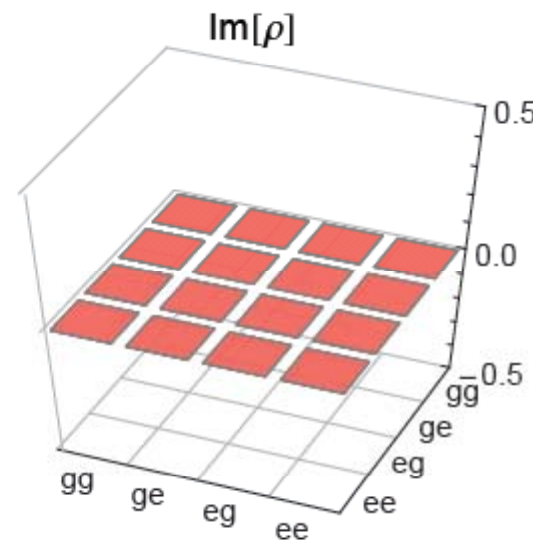
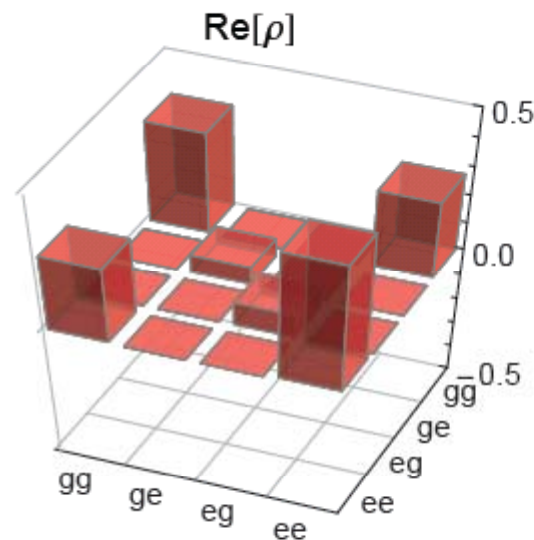
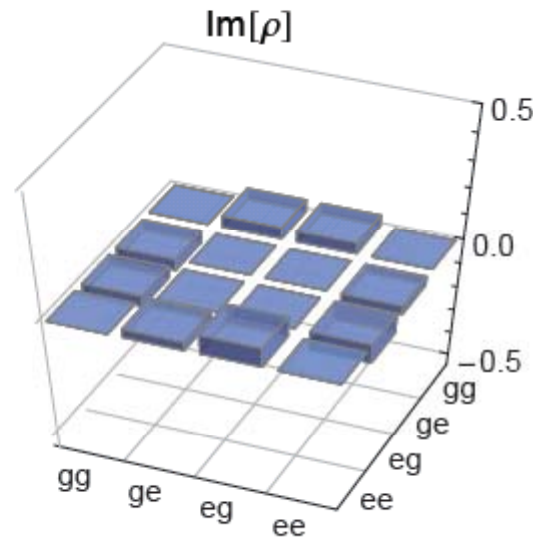
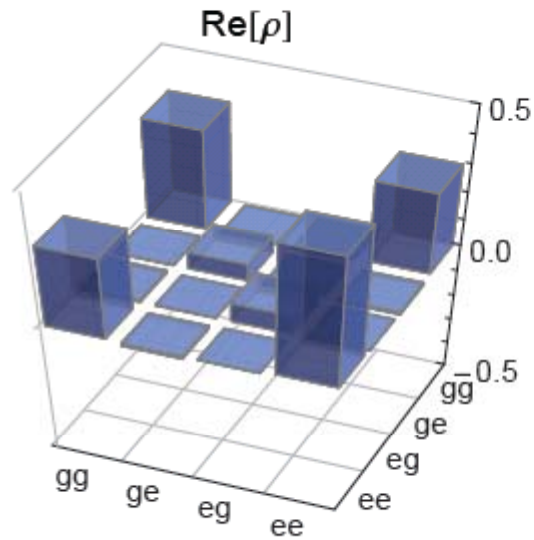
→ qubit-qubit correlations can be determined from transmission measurement

Filipp *et al.*, *Phys. Rev. Lett.* **102**, 200402 (2009)

Majer *et al.*, *Nature (London)* **445**, 443 (2007)

Blais, Huang, Wallraff, Girvin & Schoelkopf, *PRA* **69**, 062320 (2004)

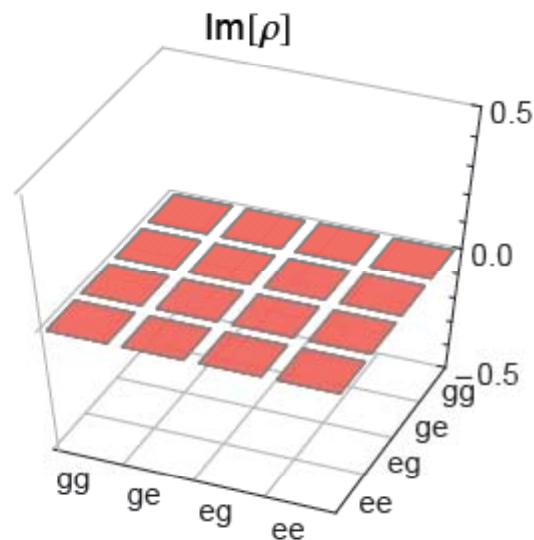
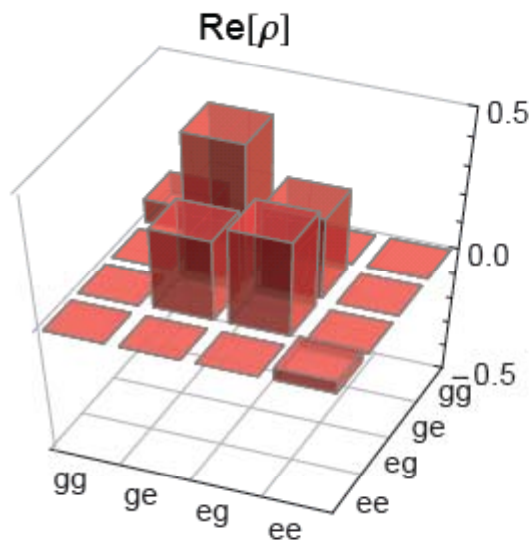
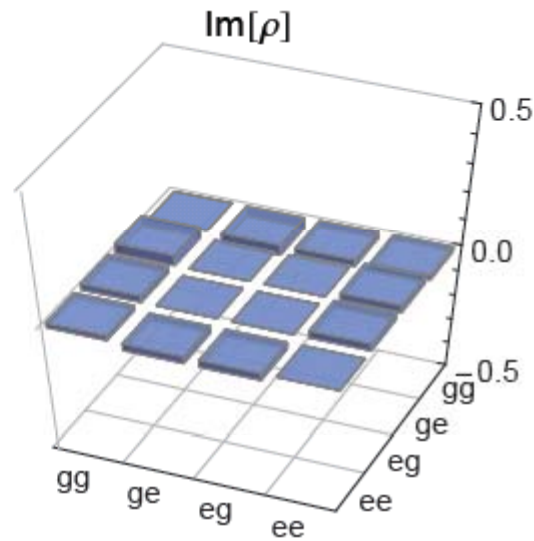
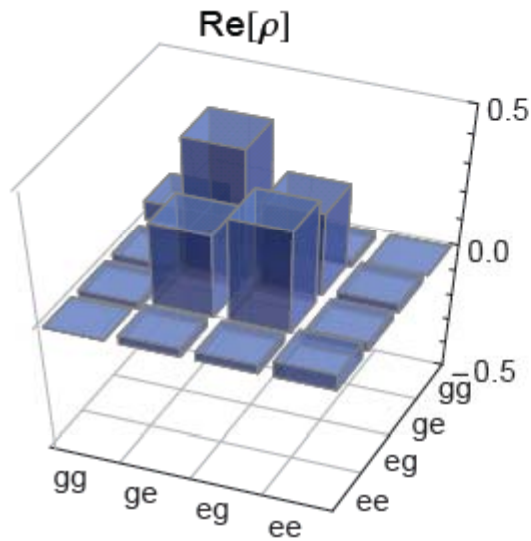
$$|\Phi_+\rangle = \frac{1}{\sqrt{2}}(|gg\rangle + |ee\rangle)$$



experimental
state fidelity:
F = 86%
concurrence:
0.541
entanglement
of formation :
0.371

overlap with
calculation
F = 99%

$$|\Psi_+\rangle = \frac{1}{\sqrt{2}}(|ge\rangle + |eg\rangle)$$



experimental
state fidelity:
F = 86%
concurrence:
0.518
entanglement
of formation :
0.374

overlap with
calculation
F = 99%

DiVincenzo Criteria fulfilled for Superconducting Qubits

for Implementing a Quantum Computer in the standard (circuit approach) to quantum information processing (QIP):

- #1. A scalable physical system with well-characterized qubits. ✓
- #2. The ability to initialize the state of the qubits. ✓
- #3. Long (relative) decoherence times, much longer than the gate-operation time. ✓
- #4. A universal set of quantum gates. ✓
- #5. A qubit-specific measurement capability. ✓

plus two criteria requiring the possibility to transmit information:

- #6. The ability to interconvert stationary and mobile (or flying) qubits. ✓
- #7. The ability to faithfully transmit flying qubits between specified locations. ✓